

Rhodium Silyl Hydrides in Oxidation State +5: Classical or Nonclassical?†

Sergei F. Vyboishchikov*‡ and Georgii I. Nikonov*§

Institut de Química Computacional, Campus de Montilivi, Universitat de Girona, 17071 Girona, Catalonia, Spain, and Chemistry Department, Brock University, 500 Glenridge Avenue, St. Catharines, Ontario, L2S 3A1, Canada

Received March 12, 2007

Four families of silyl hydride complexes of rhodium in the formal oxidation state +5 were investigated by means of DFT calculations, supplemented by the calculation of Mayer bond indices and Si–H coupling constants. In each case some degree of interligand Si–H interaction has been found. In the compounds CpRh(SiMe₃)₂H₂ (**1**), CpRh(SiMe₃)₃H (**2**), CpRh(SiMe₃)₂(SiEt₃)H (**3**), and [Cp(Me₃P)Rh(SiMe₃)₂H]⁺ (**4**) the hydride(s) interact(s) with both silyl ligands. Relaxed potential energy scans indicate that the potential energy surface is extremely flat. It takes only 1 kcal·mol⁻¹ to compress the Si–H bond from 2.3 Å to 2.0 Å in **1**, and 2 kcal·mol⁻¹ to compress the Si–H distance from 1.990 Å to 1.70 Å in complex **2**. ONIOM calculations of the compound CpRh(SiMe₃)₃H and optimization of the lowest energy conformers of complex CpRh(SiMe₃)₂(SiEt₃)H show that their geometries are largely determined by steric effects. Increasing steric hindrance promotes Si–H interactions because they result in longer Rh–Si bond lengths, leading to the relief of steric strain. The same conclusion has been drawn from the comparison of complexes [Cp(PMe₃)Rh(SiMe₃)₂H]⁺ and [Cp*(PMe₃)Rh(SiMe₃)₂H]⁺, the latter compound having stronger Si–H interactions. A very low barrier of 1.9 kcal·mol⁻¹ (on the Δ*G*₂₉₈^o scale) has been found for the hydride shift in complex **2**, accounting for its fluxionality. In contrast, the complexes [Cp(PMe₃)Rh(SiMe₃)₂H]⁺ (**4**) and [Cp(PMe₃)Rh(SiMe₃)H₂]⁺ (**8**) are not fluxional because the hydride migration is accompanied by a highly unfavorable loss of one of the Si···H interactions. The calculated Si–H coupling constants are negative when the silyl and hydride ligands are *cis* (consistent with the presence of Si–H bonding) and positive for the *trans* pairs (no Si–H bonding). The magnitude of the calculated *J*(H–Si) is in very good accord with experimental data, when the latter are available.

Introduction

Late transition metals catalyze a range of important transformations of organosilanes, including hydrosilylation of unsaturated substrates,¹ dehydrogenative coupling,^{2,3} coupling with arenes,⁴ silane alcoholysis,⁵ silane reduction of haloarenes,⁶ and

silane redistribution.⁷ These reactions are believed to proceed via Si–H bond oxidative addition to metal⁸ followed by the transformation of the silyl group in the coordination sphere of the transition metal. The formation of silyl hydride complexes

† Dedicated to Prof. Dr. Manfred Weidenbruch on the occasion of his 70th birthday.

* Corresponding authors. Fax: +34 97241 8356. Tel: +34 97241 8362. E-mail: vybo@stark.udg.es. Fax: +1 (905) 6829020. Tel: +1 (905) 6885550, ext. 3350. E-mail: gnikonov@brocku.ca.

‡Universitat de Girona.

§ Brock University.

(1) (a) Marciniak, B.; Gulinski, J.; Urbaniak, W.; Kornetka, Z. W., Eds. *Comprehensive Handbook on Hydrosilylation*; Pergamon: Oxford, 1992. (b) Roy, A.; Taylor, R. B. *J. Am. Chem. Soc.* **2002**, *124*, 9510. (c) Speier, J. L. *Adv. Organomet. Chem.* **1979**, *17*, 407. (d) Ojima, I.; Li, Z.; Zhu, J. In *The Chemistry of Organic Silicon Compounds*; Rappoport, Z., Apeloig, Y., Eds.; Wiley: New York, 1998; Vol. 2, Chapter 35, pp 1687–1792. (e) Ojima, I. In *The Chemistry of Organic Silicon Compounds*; Patai, S., Rappoport, Z., Eds.; John Wiley: Chichester, 1989; p 1479. (f) Chalk, A. J.; Harrod, J. F. *J. Am. Chem. Soc.* **1965**, *87*, 16.

(2) (a) Brook, M. A. *Silicon in Organic, Organometallic, and Polymer Chemistry*; Wiley: New York, 2000. (b) Tilley, T. D. *Acc. Chem. Res.* **1993**, *26*, 22. (c) Fontaine, F.-G.; Zargarian, D. *J. Am. Chem. Soc.* **2004**, *126*, 8786. (d) Rosenberg, L.; Davis, C. W.; Yao, J. *J. Am. Chem. Soc.* **2001**, *123*, 5120. (e) Brown-Wensley, K. A. *Organometallics* **1987**, *6*, 1590–1591. (f) Fontaine, F.-G.; Zargarian, D. *Organometallics* **2002**, *21*, 401–408.

(3) (a) Dioumaev, V. K.; Yoo, B. R.; Procopio, L. J.; Berry, D. H. *J. Am. Chem. Soc.* **2003**, *125*, 8936. (b) Procopio, L. J.; Berry, D. H. *J. Am. Chem. Soc.* **1991**, *113*, 4039.

(4) (a) Ezbiatsky, K.; Djurovich, P. I.; LaForest, M.; Sinning, D.; Zayes, R.; Berry, D. H. *Organometallics* **1998**, *17*, 1455. (b) Tsukada, N.; Hartwig, J. F. *J. Am. Chem. Soc.* **2005**, *127*, 5022.

(5) Selected publications on silane alcoholysis by late transition metals: (a) Scharrer, E.; Chang, S.; Brookhart, M. *Organometallics* **1995**, *14*, 5686. (b) Schubert, U.; Lorenz, C. *Inorg. Chem.* **1997**, *36*, 1258. (c) Lorenz, C.; Schubert, U. *Chem. Ber.* **1997**, *128*, 1267. (d) Egger, C.; Schubert, U. *Z. Naturforsch.* **1991**, *46b*, 783. (e) Luo, X.; Crabtree, R. H. *J. Am. Chem. Soc.* **1989**, *111*, 2527.

(6) (a) Alonso, F.; Beletskaya, I. P.; Yus, M. *Chem. Rev.* **2002**, *102*, 4009. (b) Karshtedt, D.; Bell, A. T.; Tilley, T. D. *Organometallics* **2006**, *25*, 4471. (c) Díaz, J.; Esteruelas, M. A.; Herrero, J.; Moralejo, L.; Oliván, M. *J. Catal.* **2000**, *195*, 187. (d) Herrero, M. A.; J.; López, F. M.; Martín, M.; Oro, L. A. *Organometallics* **1999**, *18*, 1110. (e) Boukherroub, R.; Chatgiliaoglu, C.; Manuel, G. *Organometallics* **1996**, *15*, 1508. (f) For related dehalogenation of hexachlorocyclohexanes see: Esteruelas, M. A.; Herrero, J.; Oliván, M. *Organometallics* **2004**, *23*, 3891.

(7) (a) Hashimoto, H.; Tobita, H.; Ogino, H. *J. Organomet. Chem.* **1995**, *499*, 205. (b) Rosenberg, L.; Davis, C. W.; Yao, J. *J. Am. Chem. Soc.* **2001**, *123*, 5120.

(8) Corey, J. Y.; Braddock-Wilking, J. *Chem. Rev.* **1999**, *99*, 175.

(9) (a) Cook, K. S.; Incarvito, C. D.; Webster, C. E.; Fan, Y. B.; Hall, M. B.; Hartwig, J. F. *Angew. Chem., Int. Ed.* **2004**, *43*, 5474. (b) Taw, F. L.; Bergman, R. G.; Brookhart, M. *Organometallics* **2004**, *23*, 886. (c) Okazaki, M.; Ohshitanai, S.; Tobita, H.; Ogino, H. *Chem. Lett.* **2001**, 952. (d) Nagashima, H.; Tatebe, K.; Ishibashi, T.; Nakaoka, A.; Sakakibara, J.; Itoh, K. *Organometallics* **1995**, *14*, 2868. (e) Duckett, S. B.; Perutz, R. N. *J. Chem. Soc., Chem. Commun.* **1991**, 28. (f) Duckett, S. B.; Haddleton, D. M.; Jackson, S. A.; Perutz, R. N.; Poliakoff, M.; Upmacis, R. K. *Organometallics* **1988**, *7*, 1526. (g) Fernandez, M.-J.; Maitlis, P. M. *J. Chem. Soc., Dalton Trans.* **1984**, 2063. (h) Fernandez, M.-J.; Bailey, P. M.; Bentz, P. O.; Ricci, J. S.; Koetzle, T. F.; Maitlis, P. M. *J. Am. Chem. Soc.* **1984**, *106*, 5458.

in higher formal oxidation states is, therefore, a silent feature of these reactions.

In this context, the existence of several types of silyl hydride complexes of Rh(V) is particularly noteworthy.^{4a,6b,9} The oxidation state +5 is the highest accessible stable oxidation state of rhodium, rendering the metal to be a strong oxidant.¹⁰ On this basis, one could expect that intramolecular oxidation of silyl and hydride ligands in $L_nRh^V(H)(SiR_3)$ to give silane σ -complexes¹¹ $L_nRh^{III}(\eta^2-HSiR_3)$ could open a feasible escape route toward a more favorable oxidation state of rhodium. Nevertheless, Rh(V) silyl hydrides were invoked as intermediates in Rh-mediated Si–C^{4a} and Si–Si^{9c} bond formation reactions, as precursors and intermediates in catalytic reduction of chloroarenes by $HSiEt_3$,^{6b} and as intermediates in Rh-catalyzed hydrosilylation of carbonyl compounds^{9d} and olefins.¹²

More surprisingly, several isolable, apparently Rh(V) silyl hydride complexes have been reported.⁹ In particular, Maitlis et al. reported a neutron diffraction (ND) study of the piano-stool complex $Cp^*Rh(SiR_3)_2H_2$, showing a Si–H distance of 2.27(6) Å.^{9e} Si–H distances longer than 2 Å are generally believed to be nonbonding,^{11e} allowing for the formulation of complex $Cp^*Rh(SiR_3)_2H_2$ as a formally Rh(V) compound. Earlier calculations at the Hartree–Fock level for the model complex $CpRh(SiH_3)_2H_2$ substantiated this conclusion.¹³ On the other hand, the related tri(silyl) derivatives $CpRh(SiR_3)_3H$ were reported to have some η^2 -silane character according to NMR evidence.^{9e} Nonclassical Si–H interactions were also suggested for the isoelectronic cationic complexes $[Cp^*(Me_3P)Rh(SiR_3)_2H]^+$ (R = Me, Et) characterized by increased Si–H coupling constants of 28.5 and 27.5 Hz, respectively.^{9b} The NMR properties of these apparently highly fluxional compounds were rationalized in terms of degenerate exchange between the silyl and silane ligands. For the related complexes $[Cp^*(Me_3P)Rh(SiR_3)_2H]^+$ (R = Me, Et, Ph) the assignment of a formal oxidation state of Rh turned out to be more problematic. These complexes appear to be highly fluxional and do not exhibit any measurable H–H or Si–H coupling, which does not allow one to differentiate between the Rh(III) and Rh(V) species.^{9b}

In the present work we address the following questions: Are these silyl hydride derivatives of rhodium indeed classical Rh(V) species? And if not, what kind of interligand Si···H interaction do they have? To tackle these problems, we set out to calculate a series of model compounds $[Cp(Me_3E)(X)Rh(SiMe_3)_nH]^n$ (E = Si, X = H, $n = 0$; E = Si, X = $SiMe_3$, $n = 0$; E = P, X = $SiMe_3$, $n = +1$; E = P, X = H, $n = +1$), supplemented by the calculation of Mayer indices and Si–H coupling constants. Our recent theoretical study of the isoelectronic, formally Fe(IV) complexes $Cp(L)Fe(SiR_nCl_{3-n})_2H$ (L = CO, PMe_3 ; $n = 0-3$) revealed the presence of significant interligand interactions.¹⁴

(10) Rh(VI) is known in the form of a highly unstable fluoride, RhF_6 . Rh(V) is known in the form of stable RhF_5 , which is a strong oxidant: (a) Cotton, F. A.; Wilkinson, G.; Murillo, C. A.; Bochmann, M. *Advanced Inorganic Chemistry*, 6th ed.; Wiley: New York, 1999. (b) Housecroft, C. E.; Sharpe, A. G. *Inorganic Chemistry*, 2nd ed.; Pearson: London, 2005.

(11) (a) Nikonov, G. I. *Adv. Organomet. Chem.* **2005**, *53*, 217. (b) Lin, Z. *Chem. Soc. Rev.* **2002**, *31*, 239. (c) Kubas, G. J. *Metal Dihydrogen and σ -Bond Complexes*; Kluwer Academic/Plenum: New York, 2001. (d) Crabtree, R. H. *Angew. Chem., Int. Ed. Engl.* **1993**, *32*, 789. (e) Schubert, U. *Adv. Organomet. Chem.* **1990**, *30*, 151.

(12) (a) Milan, A.; Towns, E.; Maitlis, P. M. *J. Chem. Soc., Chem. Commun.* **1981**, 673. (b) Fernandez, M.-J.; Maitlis, P. M. *J. Chem. Soc., Chem. Commun.* **1982**, 310. (c) Duckett, S. B.; Perutz, R. N. *Organometallics* **1992**, *11*, 90.

(13) Lin, Z.; Hall, M. B. *Organometallics* **1993**, *12*, 19.

(14) Vyboishchikov, S. F.; Nikonov, G. I. *Chem.–Eur. J.* **2006**, *12*, 8518.

Computational Methods

All geometry optimizations were carried out employing the density-functional theory using the Perdew–Burke–Ernzerhof exchange and correlation functionals (PBE–PBE).¹⁵ Compared to the hybrid functionals, GGA functionals, such as PBE–PBE, allow for enormous saving of computational time due to the density fitting technique.¹⁶ For rhodium, we used the “Stuttgart” effective core potential¹⁷ with the corresponding basis set (contraction scheme {311111/22111/411}). On other atoms, the standard 6-311G** basis was employed. We used a similar level of theory in our previous publications^{14,27a} and observed a good agreement with the experiment. Full geometry optimizations without symmetry constraints were performed for all the molecular structures under study. The nature of optimized stationary points was confirmed by computation of harmonic force constants.

In order to locate the energetically most stable conformer in the triethylsilyl complex **3** (*vide infra*), the following strategy was adopted. First, a reasonable conformation of **3** was optimized by DFT. Then, possible torsion angles describing the internal rotation of the ethyl groups were varied. In this manner, about 240 starting structures were generated. Subsequently, all the geometry parameters except those describing the internal rotations were frozen, and the structures were optimized using the universal force field (UFF).¹⁸ Of the resulting structures, 10 lowest nonidentical ones were chosen and reoptimized using the DFT.

The spin–spin coupling constants $J(^1H-^{29}Si)$ for the complexes under study were calculated within the gauge-including atomic orbitals (GIAO) approach¹⁹ using the Gaussian-03 program. As

(15) Perdew, J. P.; Burke, K.; Ernzerhof, M. *Phys. Rev. Lett.* **1996**, *77*, 3865.

(16) (a) Dunlap, B. I. *J. Chem. Phys.* **1983**, *78*, 3140. (b) Dunlap, B. I. *J. Mol. Struct. (THEOCHEM)* **2000**, *529*, 37.

(17) (a) Andrae, D.; Häussermann, U.; Dolg, M.; Stoll, H.; Preuss, H. *Theor. Chim. Acta* **1990**, *77*, 123. (b) <ftp://ftp.chemie.uni-karlsruhe.de/pub/basen/rh>.

(18) Rappé, A. K.; Casewit, C. J.; Colwell, K. S.; Goddard, W. A., III; Skiff, W. M. *J. Am. Chem. Soc.* **1992**, *114*, 10024–10035.

(19) Ditchfield, R. *J. Chem. Phys.* **1976**, *65*, 3123.

(20) Helgaker, T.; Watson, M.; Handy, N. C. *J. Chem. Phys.* **2000**, *113*, 9402.

(21) (a) Becke, A. D. *J. Chem. Phys.* **1993**, *98*, 5648. (b) Stephens, P. J.; Devlin, F. J.; Frisch, M. J.; Chabalowski, C. F. *J. Phys. Chem.* **1994**, *98*, 11623.

(22) Becke, A. D. *Phys. Rev. A* **1988**, *38*, 3098.

(23) (a) Lee, C.; Yang, W.; Parr, R. G. *Phys. Rev. B* **1988**, *37*, 785. (b) Miehlisch, B.; Savin, A.; Stoll, H.; Preuss, H. *Chem. Phys. Lett.* **1989**, *157*, 200.

(24) Kutzelnigg, W.; Fleischer, U.; Schindler, M. In *NMR Basic Principles and Progress*; Diehl, P., Fluck, E., Günther, H., Kosfeld, R., Seelig, J., Eds.; Springer: Berlin, 1990; Vol. 23, p 165.

(25) Frisch, M. J.; et al. *Gaussian 03*, Revision D.01; Gaussian, Inc.: Wallingford, CT, 2004.

(26) For leading references on the calculation of NMR chemical shifts and coupling constants see: (a) Autschbach, J. The calculation of NMR parameters in transition metal complexes. In *Principles and Applications of Density Functional Theory in Inorganic Chemistry I*; Kaltsoyannis, N., McGrady, J. E., Eds.; Springer: Heidelberg, 2004; Vol. 112. (b) Autschbach, J.; Ziegler, T. Relativistic calculation of spin-spin coupling constants. In *Calculation of NMR and EPR Parameters. Theory and Applications*; Kaupp, M., Bühl, M., Malkin, V. G., Eds.; Wiley-VCH: Weinheim, 2004. (c) Autschbach, J.; Ziegler, T. Relativistic computation of NMR shieldings and spin-spin coupling constants. In *Encyclopedia of Nuclear Magnetic Resonance*; Grant, D. M., Harris, R. K., Eds.; John Wiley & Sons: Chichester, 2002; Vol. 9. (d) Le Guennic, B.; Patchkovskii, S.; Autschbach, J. *J. Chem. Theory Comput.* **2005**, *1*, 601, and references therein. (e) Solans-Monfort, X.; Eisenstein, O. *Polyhedron* **2006**, *25*, 339–348, and references therein.

(27) (a) Osipov, A. L.; Vyboishchikov, S. F.; Dorogov, K. Y.; Kuzmina, L. G.; Howard, J. A. K.; Lemenovskii, D. A.; Nikonov, G. I. *Chem. Commun.* **2005**, 3349. (b) Ignatov, S. K.; Rees, N. H.; Tyrrell, B. R.; Dubberley, S. R.; Razuvaev, A. G.; Mountford, P.; Nikonov, G. I. *Chem.–Eur. J.* **2004**, *10*, 4991. (c) Lichtenberger, D. L. *Organometallics* **2003**, *22*, 1599. (d) Pandey, K. K.; Lein, M.; Frenking, G. *Organometallics* **2004**, *23*, 2944.

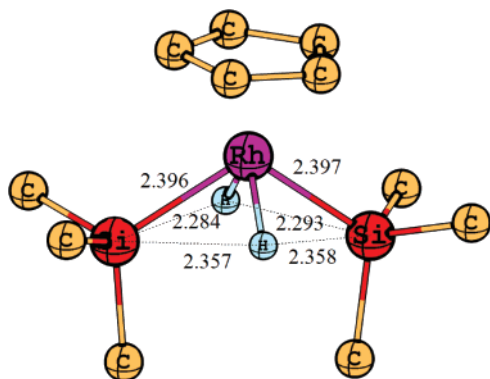


Figure 1. Structure of complex $\text{CpRh}(\text{SiMe}_3)_2\text{H}_2$ (**1**). Non-hydride hydrogen atoms are omitted for clarity. Distances are given in ångströms.

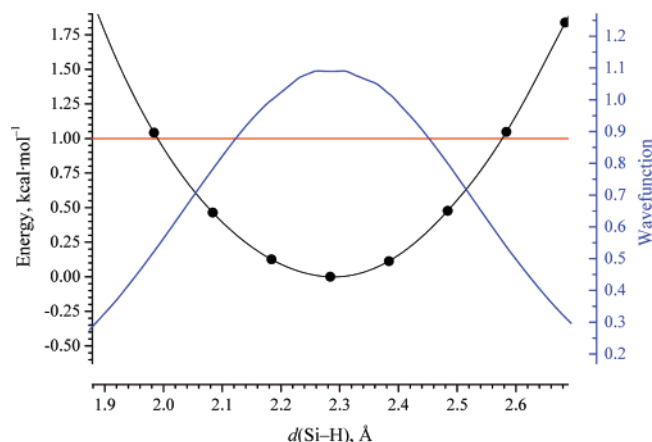


Figure 2. Relaxed scan of the potential energy surface of hydride motion in complex **1** (black curve) and the corresponding one-dimensional vibrational ground-state wavefunction (blue curve). The red bar denotes the level of 1 kcal·mol⁻¹. The ground-state vibrational energy is 0.7 kcal·mol⁻¹.

hybrid functionals were shown to perform more reliably for spin-spin coupling constants,²⁰ the NMR parameters were calculated using B3LYP,²¹ the hybrid functional combining Becke's nonlocal exchange²² with Hartree-Fock exchange along with the Lee-Yang-Parr correlation functional.²³

Taking into account the high sensitivity of magnetic values to the basis set and to the density functional, more extended basis sets for silicon and hydrogen were used for the NMR calculations. These correspond to the completely decontracted "IGLO-III" basis set of Kutzelnigg and co-workers.²⁴ To provide better flexibility in the core region, which is important for coupling constants,²⁰ it was augmented by one steep *s*-function at silicon and hydrogen. On other atoms, the original basis used for optimization was retained.

All the calculations in the present work were performed with the Gaussian 03 program package,²⁵ with the exception of vibrational wavefunction calculations (*vide infra*).

Results and Discussion

1. CpRh(SiMe₃)₂H₂. The optimized structure of complex $\text{CpRh}(\text{SiMe}_3)_2\text{H}_2$ (**1**) is shown in Figure 1. This is a piano-stool complex having a pair of *trans* silyl ligands and a pair of *trans* hydrides. The computed Rh-Si bond distances are almost identical (2.397 and 2.396 Å) and close to the experimental value (2.379(2) Å) obtained for the compound $\text{Cp}^*\text{Rh}(\text{SiEt}_3)_2\text{H}_2$.^{9h} The four Si-H distances fall into the range 2.284–2.358 Å (Table 1), which compares well with the average distance of 2.27(6) Å observed by the neutron diffraction. Si-H distances of such

Table 1. $J(^1\text{H}-^{29}\text{Si})$ Spin-Spin Coupling Constants, Si···H Distances, and Si···H Mayer Bond Indices

molecule	$J(^1\text{H}-^{29}\text{Si})$, Hz	Si···H distance, Å	Si···H Mayer bond index
1			
H(1)-Si(1)	-3.4	2.293	0.11
H(1)-Si(2)	-4.0	2.284	0.11
H(2)-Si(1)	-1.1	2.358	0.09
H(2)-Si(2)	-1.5	2.357	0.09
2	average: -8.1		
H-Si(1)	-20.6	1.995	0.18
H-Si(2)	-12.7	2.073	0.14
H-Si(3)(<i>trans</i>)	+9.1	3.058	-0.01
3a	average(SiMe ₃): -4.0		
H-SiEt(<i>cis</i>)	-23.4	1.996	0.18
H-SiMe(<i>cis</i>)	-12.1	2.128	0.15
H-SiMe(<i>trans</i>)	+4.1	3.066	-0.01
3a'	average(SiMe ₃): -6.9		
H-SiEt(<i>cis</i>)	-24.4	1.998	0.16
H-SiMe(<i>cis</i>)	-17.7	2.085	0.13
H-SiMe(<i>trans</i>)	+4.0	3.022	-0.01
3b	average(SiMe ₃): -24.3		
H-SiMe(<i>cis</i> 1)	-29.4	1.967	0.18
H-SiMe(<i>cis</i> 2)	-19.1	2.046	0.14
H-SiEt(<i>trans</i>)	+4.6	3.018	-0.02
4	average: -14.9		
H-Si(1)	-18.5	2.008	0.15
H-Si(2)	-11.3	2.083	0.10
5	average: -29.6		
H-Si(1)	-64.4	1.682	0.38
H-Si(2)	+5.3	2.679	-0.01
6	average: -27.5		
H-Si(1)	-33.8	1.909	0.20
H-Si(2)	-11.1	2.099	0.11
7	average: -42.1		
H-Si(1)	-86.8	1.598	0.57
H-Si(2)	+2.6	2.752	0.02
8	average: -8.4		
H-Si(1)	-11.5	2.096	0.14
H-Si(2)	-5.3	2.240	0.10

length are usually interpreted as nonbonding,^{11e} leading to the formulation of this compound as a Rh(V) species. There is an asymmetry in the structure, with one hydride forming somewhat shorter Si···H contacts (2.293 and 2.284 Å) than the other (2.358 and 2.357 Å).

The calculation of silicon-hydride coupling constants by means of quantum chemistry is potentially an attractive alternative to experiment,²⁶ particularly when the $J(\text{Si}-\text{H})$ cannot be determined due to the width of the ²⁹Si and ¹H NMR signals. In a few cases, when both the calculated and experimental data are available, a fair agreement has been observed.^{14,27} The Si-H coupling constants for the complex $\text{Cp}^*\text{Rh}(\text{SiEt}_3)_2\text{H}_2$ have not been reported. The calculated $J(\text{H}-\text{Si})$ values for the model compound **1** are found in the range -1.1 to -4.0 Hz (Table 1). Although the absolute values are small, the negative signs indicate that there could be some residual Si-H bonding in this complex,^{27b} with each hydride interacting simultaneously and with a similar strength with both *cis* silyl ligands. Indeed, the calculated Mayer indices²⁸ fall in the range 0.09 to 0.11 (Table 1). Compared to a Si-H Mayer index of 0.92 in HSiMe_3 , this suggests a very weak Si-H bonding.

To check the sensitivity of the molecular energy of **1** with respect to the hydride position, we performed a relaxed scan of the potential energy surface. To this end, the Si···H distance was frozen at different values, while all other geometry parameters were optimized. The dependence of the energy on the Si···H distance is shown in Figure 2. Most importantly, the potential energy surface is extremely shallow. The hydride can

(28) Mayer, I. *Chem. Phys. Lett.* **1983**, *97*, 270; addendum **1985**, *99*, 117.

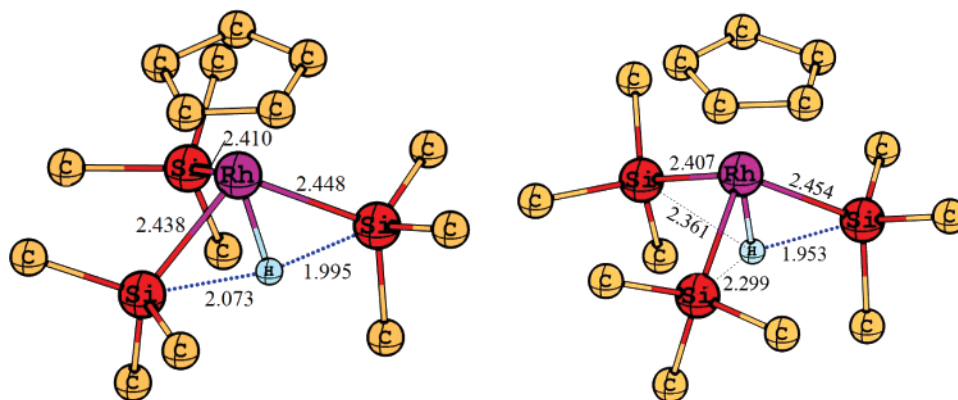


Figure 3. Structure of complex $\text{CpRh}(\text{SiMe}_3)_3\text{H}$ (**2**, left-hand side) and the transition state for the hydride wandering (TS, right-hand side). Non-hydride hydrogen atoms are omitted for clarity. Distances are given in ångströms.

be moved as far from its equilibrium position as 0.3 Å, with the energy cost of only 1 kcal·mol⁻¹. Such a situation is not unusual in the field of nonclassical compounds, being sometimes observed for elongated dihydrogen complexes.²⁹ It can be expected that on such a flat surface the hydride can move broadly. To quantify this conjecture, we solved the one-dimensional vibrational Schrödinger equation for the motion of a free hydrogen atom in the calculated potential. This calculation was performed variationally in a basis of 40 one-dimensional harmonic oscillator eigenfunctions centered at the minimum position of the potential (at the Si···H distance of 2.284 Å) using a program written by the authors. For the vibrational ground state, this technique provides a nearly exact solution of the Schrödinger equation (within the given one-dimensional potential). Of course, this approach has some limitations, since it neglects the coupling of hydride motion with that of other atoms. Nevertheless, it is certainly justified for semiquantitative purposes. The resulting ground-state vibrational wavefunction $\Psi(r)$ (blue curve in Figure 2) is indeed substantially delocalized in a broad area around the minimum. Numerical integration of $|\Psi(r)|^2$ shows that the likelihood of finding the hydride farther away from the equilibrium position by 0.15 Å is about 35%, while finding it away from the equilibrium by 0.3 Å is still about 7%. Therefore, we indeed encounter a hydride ligand that will be significantly delocalized even at 0 K. This situation is typical of complexes described in the present work.

In conclusion, although the minimum energy structure of $\text{CpRh}(\text{SiMe}_3)_2\text{H}_2$ (**1**) appears to be consistent with its description as a nearly Rh(V) silylhydride complex, the extremely flat potential for the residual Si–H interaction calculated for this compound shows that the formalism of oxidation states loses its meaning for this system.

2. CpRh(SiMe₃)₃H (2). Substitution of a hydride ligand in **1** for the SiMe₃ group affords an isoelectronic complex $\text{CpRh}(\text{SiMe}_3)_3\text{H}$. Calculation of this compound afforded a distorted piano-stool structure (Figure 3), in which the hydride deviates only slightly from the Rh(*cis*-SiMe₃)₂ plane defined by Rh and two silyl group *cis* to hydride (Si–Rh–H–Si dihedral angle is 169.5°). A similar type of distortion has been previously found

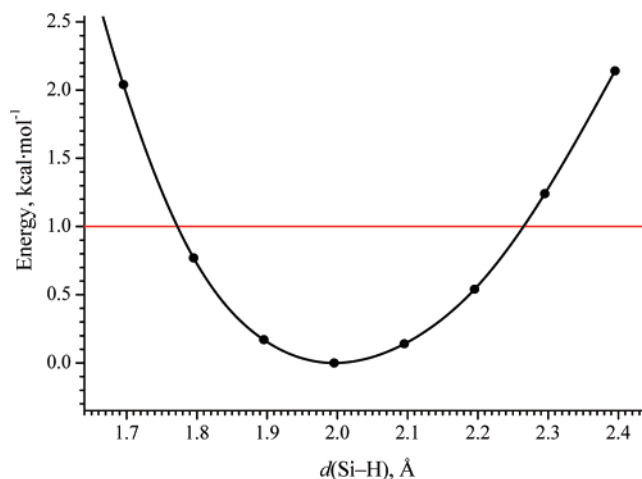


Figure 4. Relaxed scan of the potential energy surface of hydride motion in complex **2**. Potential energy values are given in kcal·mol⁻¹. The red bar denotes the level of 1 kcal·mol⁻¹.

for the isoelectronic compound $\text{Cp}(\text{Me}_3\text{P})\text{Fe}(\text{SiMe}_3)_2\text{H}$ with nonclassical interligand interactions between the central hydride and two lateral silyl groups (Si–H distances of 1.996 and 1.955 Å).¹⁴ The calculated Si–H contacts to the *cis* silyls in **2** are 1.990 and 2.058 Å, which suggests that a similar kind of Si–H bonding can also be present in **2**. Indeed, these short Si–H contacts correspond to significant Mayer indices of 0.14 and 0.18, respectively (Table 1). As a further signature of the presence of nonclassical Si–H bonding, the silicon atoms located *cis* to the hydride have longer Rh–Si bond lengths (2.438 and 2.448 Å) than the silyl *trans* to the hydride (2.410 Å), with the shorter Si–H distance corresponding to a longer Rh–Si bond. The Rh–Si(*cis*) bond exhibits lower Mayer indices than the Rh–Si(*trans*) bond and than the Rh–Si bonds in complex **1** (see Table 2). The *trans* Rh–Si bond compares well with the values observed for **1** both in terms of distances (2.396 and 2.397 Å) and Mayer indices (0.76 versus 0.73). In silane σ -complexes, longer than normal M–Si distances are usually observed,¹¹ although recent studies indicate that the correlation between the M–Si distance and the extent of Si–H interaction may be not straightforward.³⁰ The multicentral Si–H interactions^{11a} described here and previously in the iron complexes $\text{Cp}(\text{L})\text{Fe}(\text{SiR}_3)_2\text{H}$ ¹⁴ are also characterized by somewhat longer M–Si bond lengths.

(29) (a) Heinekey, D. M.; Lledós, A.; Lluch, J. M. *Chem. Soc. Rev.* **2004**, 33, 175. (b) Barea, G.; Esteruelas, M.; Lledós, A.; López, A. M.; Tolosa, J. L. *Inorg. Chem.* **1998**, 37, 5033. (c) Gelabert, R.; Moreno, M.; Lledós, A.; Lluch, J. M. *J. Am. Chem. Soc.* **1997**, 119, 9840. (d) Gelabert, R.; Moreno, M.; Lluch, J. M.; Lledós, A.; Pons, V.; Heinekey, D. M. *J. Am. Chem. Soc.* **2004**, 126, 8813. (e) Gelabert, R.; Moreno, M.; Lluch, J. M.; Lledós, A.; Heinekey, D. M. *J. Am. Chem. Soc.* **2005**, 127, 5632. (g) Gusev, D. G. *J. Am. Chem. Soc.* **2004**, 126, 14249. (h) Gelabert, R.; Moreno, M.; Lluch, J. M. *Chem.–Eur. J.* **2005**, 11, 6315.

(30) (a) Nikonov, G. I. *Organometallics* **2003**, 22, 1597. (b) Ignatov, S. K.; Rees, N. H.; Dubberley, S. R.; Razuvaev, A. G.; Mountford P.; Nikonov, G. I. *Chem. Commun.* **2004**, 952.

Table 2. Ru–Si and Ru–H Mayer Bond Indices

molecule	Mayer bond index
1	
Rh–H1	0.71
Rh–H2	0.74
Rh–Si1	0.73
Rh–Si2	0.73
2	
Rh–H	0.60
Rh–Si1	0.66
Rh–Si2	0.70
Rh–Si3(<i>trans</i>)	0.76
3a	
Rh–H	0.58
Ru–SiEt(<i>cis</i>)	0.65
Ru–SiMe(<i>cis</i>)	0.67
Ru–SiMe(<i>trans</i>)	0.77
3a'	
Rh–H	0.61
Ru–SiEt(<i>cis</i>)	0.69
Ru–SiMe(<i>cis</i>)	0.69
Ru–SiMe(<i>trans</i>)	0.77
3b	
Rh–H	0.59
Rh–SiMe(<i>cis</i> 1)	0.67
Rh–SiMe(<i>cis</i> 2)	0.70
Rh–SiEt(<i>trans</i>)	0.80
4	
Rh–H	0.64
Ru–Si(1)	0.61
Ru–Si(2)	0.64
5	
Rh–H	0.52
Ru–Si(1)	0.76
Ru–Si(2)	0.35
6	
Rh–H	0.61
Ru–Si(1)	0.56
Ru–Si(2)	0.65
7	
Rh–H	0.36
Rh–Si(1)	0.13
Rh–Si(2)	0.76
8	
Rh–H(1)	0.71
Rh–H(2)	0.75
Rh–Si(1)	0.59

To establish the shape of the Si–H–Si potential and to understand the origin of asymmetry in the Si–H bonding in **2**, we performed a series of relaxed scans of the potential energy surface. Varying the Si–H distance in the range 1.5–2.4 Å provided a very shallow asymmetric single-well potential (Figure 4), similar to that described above for complex **1**. It takes less than 2 kcal·mol⁻¹ to compress the Si–H distance from the minimum value of 1.99 Å to 1.70 Å, which is a characteristic distance in silane σ -complexes.¹¹ On the other hand, another relaxed scan shows that internal rotation of the SiMe₃ group closest to the hydride by 60° around the Rh–Si axis leads to an increase of the Si–H distance from 1.990 Å to 2.047 Å. Simultaneously, the distance between the hydride and the farther silicon shortens from 2.077 Å to 2.049 Å, with the total energy increasing by 3.7 kcal·mol⁻¹. Such a rotation, corresponding to placing a methyl group from the position *trans* to the Cp to the *cis* position, is accompanied by the elongation of the Rh–Si bond from 2.448 Å to 2.460 Å. Similarly, a rotation of the silyl group *trans* to the hydride also affects the extent of Si···H interaction through the change of intersilyl steric interactions, leading to the variation of the Si–H distance in the range 1.940–2.101 Å. We therefore conclude that it is the librational motion of silyl groups that provides a mechanism for hydride transfer from a position closer to one silyl to a position closer to the other one. This librational motion controls the strength

of Si···H interaction in this system and depends in turn on the extent of steric interaction between the bulky ligands (the Cp and silyls).

To verify the effect of sterics on the strength of Si–H bonding, we decided to use the ONIOM method³¹ as implemented in Gaussian 03.³² Normally, ONIOM and other combined QM/MM schemes are applied in order to describe inexpensively the steric bulk of a large molecule using a force field, while a chemically important part of the molecule is covered by a quantum mechanical method. Here, we made use of a side effect of this approach, which allows us to separate electronic and steric effects. In particular, we model the methyl groups of **2** by using the universal force field,¹⁸ imposing hydrogens as link atoms. This leads to CpRh(SiH₃)₃H as a model quantum mechanical system. Although the steric effects of the SiMe₃ ligands are retained, electronically they act as SiH₃ ligands, which are presumably less electron donating.

The ONIOM(PBEPBE:UFF) optimization resulted in a structure that is only slightly different from the DFT-optimized one. The Si···H distances are more symmetric in the ONIOM structure (2.023 and 2.036 Å compared to 1.995 and 2.073 Å in the DFT structure). Both the Rh–Si bonds elongate slightly (by 0.01–0.02 Å), while the Rh–H bond remains untouched. The hydride lies in the plane of the *cis* silyl ligands in the DFT structure (the Si–Rh–H–Si dihedral angle is 179.8°) and deviates slightly from it in the ONIOM structure (the Si–Rh–H–Si dihedral angle is 169.5°). This result should be compared with the fully optimized structure of the model complex CpRh–(SiH₃)₃H (**2'**). The latter exhibits short Rh–Si bonds (about 2.39 Å each), quite long Si···H distances (2.179 and 2.147 Å), and a Si–Rh–H–Si dihedral angle of 135.7°. In brief, CpRh–(SiH₃)₃H has a typical four-legged piano-stool structure. On the basis of the comparison of these three structures, we see that the geometry of CpRh(SiMe₃)₃H is largely determined by steric effects.

The H–Si coupling constants calculated for **2** are –20.6 and –12.7 Hz for the *cis* silyls and +9.1 Hz for the *trans* SiMe₃ ligand. The negative $J(\text{H–Si})$ to the *cis* silyls supports the presence of direct bonding.^{27b} The average Si–H coupling (–8.1 Hz) is in good agreement with the experimental value of |13.5| Hz. Complex CpRh(SiMe₃)₃H gives rise to equivalent ¹H, ¹³C, and ²⁹Si NMR resonances of the silyl groups even at 197 K, suggesting a rapid exchange process.^{9c} If one considers complex **2** as a pseudo-octahedron CpRh(SiMe₃)₃ (with Cp occupying three coordination sites) capped on the Si–Si edge by a hydride, such an exchange can be viewed as hydride wandering from one edge to another on the RuSi₃ facet. We calculated a transition-state structure (**TS**) for this exchange, which is best described as a distorted trigonal bipyramid with apical Cp and H ligands (Figure 3, right). This **TS** appears to have a silane σ -complex character, with one H–Si distance being much shorter (1.923 Å) than the two others (2.299 and 2.361 Å). Obviously, a stronger Si–H interaction with one of the silyls in the **TS** facilitates the exchange. The calculated ΔE_c barrier of only 2.6 kcal·mol⁻¹ (1.9 kcal·mol⁻¹ on the ΔG_{298}° scale) accounts for the observed fluxionality of this system.

In conclusion, complex **2** is not a silane σ -complex; rather it has delocalized Si–H interactions between the hydride and two *cis* silyl ligands. Silyl groups exchange rapidly due to very facile shift of the hydride between different Si–Si edges of the CpRh–(SiMe₃)₃ fragment, giving rise to fluxional NMR spectra even at very low temperature.

(31) Maseras, F.; Morokuma, K. *J. Comput. Chem.* **1995**, *16*, 1170.(32) Vreven, T.; Morokuma, K. *J. Comput. Chem.* **2000**, *21*, 1419.

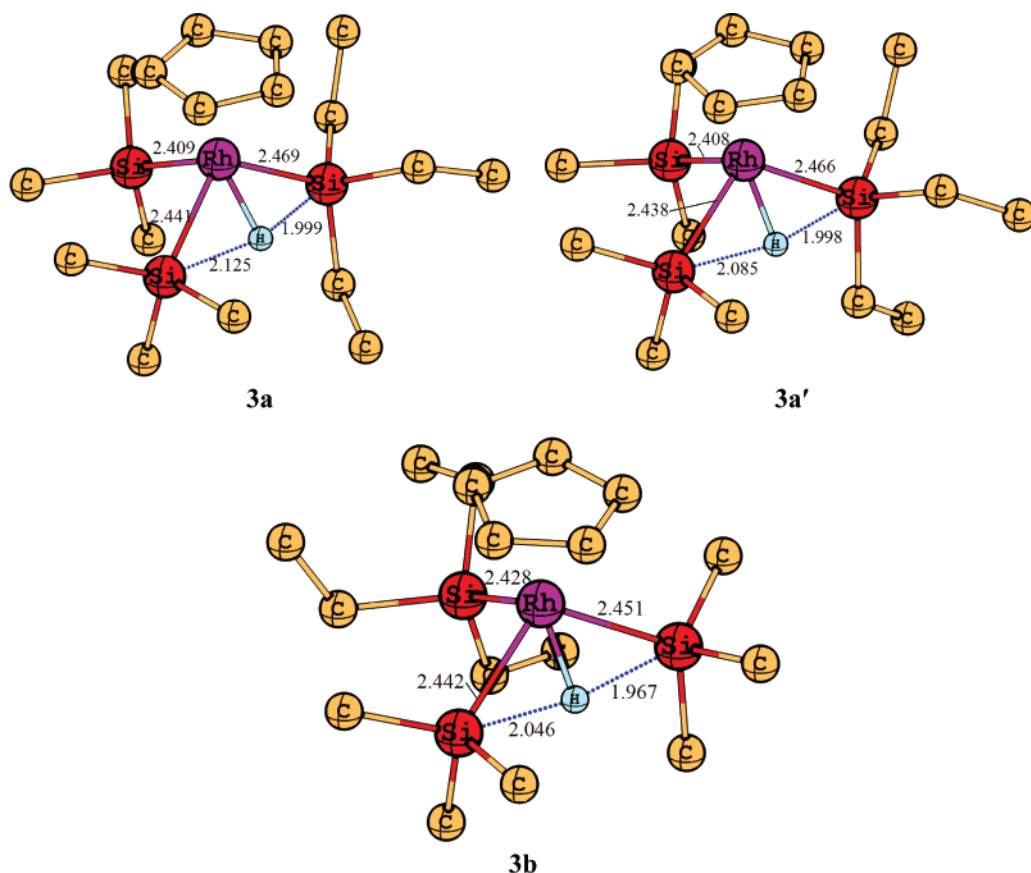


Figure 5. Structures of various configurations of the complex $\text{CpRh}(\text{SiMe}_3)_2(\text{SiEt}_3)\text{H}$ (**3**). **3a** and **3a'** are the two most stable conformers differing in the conformation of the ethyl group. **3b** has the hydride on the $\text{Me}_3\text{Si}-\text{SiMe}_3$ edge. Non-hydride hydrogen atoms are omitted for clarity. Distances are given in ångströms.

3. $\text{CpRh}(\text{SiMe}_3)_2(\text{SiEt}_3)\text{H}$ (3**).** Complex **3** is the exact model of a real compound studied by Duckett and Perutz.^{9e} Like the related compound **2**, it shows equivalent ^1H , ^{13}C , and ^{29}Si NMR resonances of the SiMe_3 groups. We calculated two structural isomers of **3**, one with the hydride on the $\text{Me}_3\text{Si}-\text{SiEt}_3$ edge (**3a**) of the pseudo-octahedral fragment $\text{CpRh}(\text{SiMe}_3)_2(\text{SiEt}_3)$ and another one with the hydride on the $\text{Me}_3\text{Si}-\text{SiMe}_3$ edge (**3b**) (Figure 5). In both cases the hydride is found in close proximity to two silyl groups but, as in **2**, is positioned asymmetrically on the Si-Si edge. In the isomer **3b**, which is $4 \text{ kcal}\cdot\text{mol}^{-1}$ less stable than **3a**, the H-Si distances are 1.967 and 2.046 Å. In the isomer **3a**, the H-SiEt₃ distance is 1.999 Å and the H-SiMe₃ distance is 2.125 Å. In **3a**, a stronger Si-H interaction corresponds to a longer Rh-Si bond: 2.469 versus 2.441 Å.

A careful conformational search (see the Computational Methods section above) revealed four more conformers of **3a** within $2 \text{ kcal}\cdot\text{mol}^{-1}$, differing in the orientation of the ethyl groups within the SiEt_3 ligand. In all these structures the hydride is found closer to the SiEt_3 group. The lowest conformer (next to **3a**) is also shown in Figure 4 as **3a'**. It lies $0.6 \text{ kcal}\cdot\text{mol}^{-1}$ higher in electronic energy than **3a** and is even $0.2 \text{ kcal}\cdot\text{mol}^{-1}$ more stable than **3a** in terms of ΔG_{298}° . In **3a'**, the Rh-Si bonds as well as the $\text{H}\cdots\text{SiEt}_3$ distance are virtually the same as in **3a**, while the $\text{H}\cdots\text{SiMe}_3$ distance is markedly shorter (2.085 Å in **3a'** versus 2.125 Å in **3a**).

The calculated H-Si coupling constants in **3a** are close to the values found for **2**: -23.4 Hz for the *cis* SiEt_3 ligand and -12.1 Hz for the *cis* SiMe_3 . In **3a'** the $J(\text{H}-\text{Si})$ of -24.4 Hz for the SiEt_3 group is quite comparable with that of the SiMe_3 group (-17.7 Hz), in spite of the difference in Si-H distances,

which may reflect the preference for the hydride to interact with the bulkier silyl substituent. It is also noteworthy that in the isomer **3b** both *cis* silyls have larger $J(\text{H}-\text{Si})$ than in **2** (-29.4 and -19.1 Hz), whereas coupling to the *trans* SiEt_3 group is diminished ($+4.6 \text{ Hz}$). Such a difference can be a result of a decreased $\text{Me}_3\text{Si}-\text{Rh}-\text{SiMe}_3$ bond angle in **3b** (109.6° versus 111.1° in **2**) caused by the repulsion from the bulkier *trans* SiEt_3 group. The coupling constant $J(\text{H}-\text{SiEt}_3)$, averaged according to the Boltzmann distribution,³³ is -23.9 Hz and the thermally averaged $J(\text{H}-\text{SiMe}_3)$ is -5.0 Hz , which is in excellent agreement with experimental values of $|24.3|$ and $|6.0| \text{ Hz}$, respectively.^{9e}

In conclusion, compound **3**, like the related complex **2**, exhibits delocalized $\text{Si}\cdots\text{H}$ interactions between the hydride and two *cis* silyl ligands. The bulkier SiEt_3 group prefers to occupy a position *cis* to the hydride, which results in longer Rh-Si bonds and more effective relief of steric strain. A similar idea, expressed in terms of silane σ -complex theory, has been previously suggested by Duckett and Perutz.^{9e}

4. $[\text{CpRh}(\text{SiMe}_3)_2(\text{PMe}_3)\text{H}]^+$ (4**).** We then turned to the isoelectronic complex $[\text{CpRh}(\text{SiMe}_3)_2(\text{PMe}_3)\text{H}]^+$, which is a model of the compound $[\text{Cp}^*\text{Rh}(\text{SiMe}_3)_2(\text{PMe}_3)\text{H}]^+$ studied in solution by NMR spectroscopy.^{9b} The latter complex exhibits equivalent silyl signals in the ^1H NMR down to -60°C and a hydride signal flanked by ^{29}Si satellites (28.5 Hz). These observations were rationalized in terms of a fast degenerate exchange between two forms of a Rh(III) η^2 -silane complex:

(33) Atkins, P.; de Paula, J. *Atkins' Physical Chemistry*, 7th ed.; Oxford, 2002; p 632.

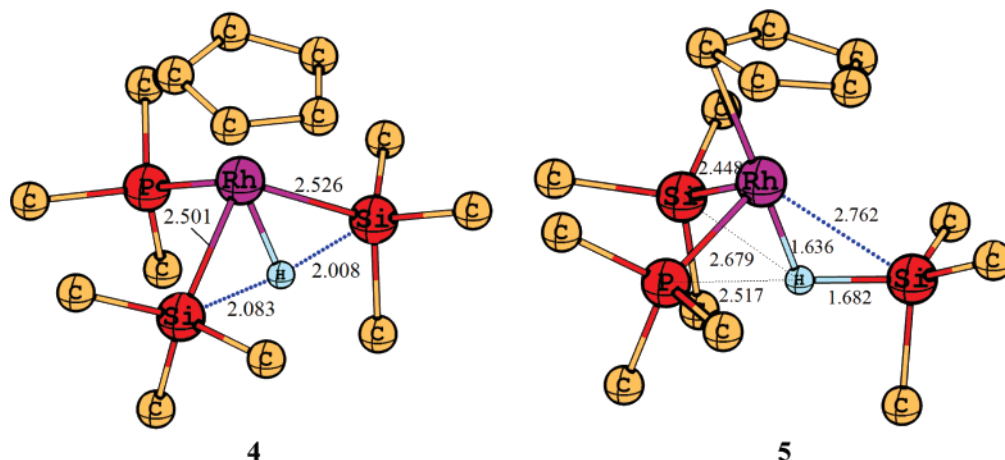


Figure 6. Structures of the bis(silyl) hydride cation complex $[\text{CpRh}(\text{SiMe}_3)_2(\text{PMe}_3)\text{H}]^+$ (**4**) and the silyl silane cation σ -complex $[\text{Cp}(\text{PMe}_3)\text{Rh}(\eta^2\text{-H-SiMe}_3)(\text{SiMe})]^+$ (**5**). Non-hydride hydrogen atoms are omitted for clarity. Distances are given in ångströms.

$[\text{Cp}^*(\text{Me}_3\text{P})\text{Rh}(\eta^2\text{-HSi}^a\text{Me}_3)(\text{Si}^b\text{Me})]^+ \rightleftharpoons [\text{Cp}^*(\text{Me}_3\text{P})\text{Rh}(\text{Si}^a\text{Me}_3)(\eta^2\text{-H-Si}^b\text{Me})]^+.$ ^{9b}

Computationally, we found two isomers of the complex $[\text{CpRh}(\text{SiMe}_3)_2(\text{PMe}_3)\text{H}]^+$: one is an analogue of complexes **2** and **3** with the hydride *trans* to the phosphine (**4**) (Figure 6, left), and another is a silyl silane σ -complex $[\text{Cp}(\text{PMe}_3)\text{Rh}(\eta^2\text{-H-SiMe}_3)(\text{SiMe})]^+$ (**5**) (Figure 6, right). The latter form was obtained from optimization of a structure with the hydride capping the P–Si edge of the complex. The silane complex **5** was found to lie rather high in energy (5.7 kcal·mol⁻¹ above **4**) and thus is not significantly populated at room temperature and below. Interestingly, in **5** the hydride is placed inside the triangle Si₂P rather than residing on the Si–P edge of a hydride capped pseudo-octahedron CpRh(SiMe₃)₂(PMe₃). This leads to the best description of **5** as a three-legged piano-stool complex, with the silane occupying one of the legs. Consistent with this description, the hydride is placed nearly equidistantly from the farthest silyl group (2.679 Å) and the phosphine ligand (2.517 Å). The short Si–H distance of 1.682 Å is indicative of a strong bonding, characteristic of silane σ -complexes. As expected, the Rh–Si bond length to the silane ligand is noticeably longer than the Rh–silyl distance (2.762 versus 2.448 Å). Overall, there is strong resemblance between the minimum energy structure of **5** and the **TS** of hydride migration in **2** discussed above.

The most stable isomer **4** is structurally similar to the tris(silyl) complexes **2** and **3** described above. Like the latter compounds, it has two relatively short Si–H contacts (2.008 and 2.083 Å), with the shorter Si–H distance corresponding to the longer Rh–Si bond (2.526 versus 2.501 Å). Both these Rh–Si distances are markedly longer than the rhodium–silyl bond length in complex **5**. The interaction with the central hydride, which manifests itself in Mayer indices (0.15 and 0.10 for the Si···H interaction), appears to be the reason for the elongation.

The Mayer index for the Rh–H bond in **4** is slightly larger than in **2**, which can be explained by the strengthening hydride bond due to the presence of a positive charge.³⁴ However, this effect is not reflected in the Rh–H distance, which is even slightly longer in **4** than in **2** (1.586 versus 1.582 Å).

The calculation of H–Si coupling constants in **4** afforded –11.3 and –18.5 Hz. The average value of –14.9 Hz is about twice less than the experimental coupling constant of |27.5| Hz obtained by Taw, Bergman, and Brookhard.^{9b} For the silane complex **5**, a $J(\text{H-Si})$ of –64.4 Hz was found for the coupling

within the η^2 -silane ligand and +5.3 Hz for the coupling between the hydride and silyl ligands. As expected, direct bonding corresponds to a negative coupling constant, whereas nonbonding magnetic interaction results in a positive $J(\text{H-Si})$.^{27b}

To determine the effect of ring substitution on the extent of Si–H interaction, the structure of the real pentamethylcyclopentadienyl-containing cation $[\text{Cp}^*\text{Rh}(\text{SiMe}_3)_2(\text{PMe}_3)\text{H}]^+$ was optimized. The effect of substitution is not *a priori* obvious because, on one hand, the Cp* ligand is a stronger electron donor and should lead to more effective back-donation from the metal, eventually weakening the Si–H bonding.^{11c} On the other hand, the large steric hindrance exerted by the Cp* ring can push the SiMe₃H moiety away from the metal, thus promoting Si–H interaction. Again, as in the case of unsubstituted complex $[\text{CpRh}(\text{SiMe}_3)_2(\text{PMe}_3)\text{H}]^+$, two isomers were found. The most stable form is the bis(silyl) complex **6** (Figure 7, left). Compared with the analogue **4**, **6** has a stronger Si–H interaction with one of the silyl ligands, evidenced by a shorter Si–H bond (the shortest Si···H distance in **6** is 1.909 Å versus 2.008 Å in **4**), larger Si···H Mayer indices (0.20 in **6** compared to 0.15 in **4**, Table 1), and longer Rh–Si bond (2.562 versus 2.526 Å) with a lower Mayer index (0.56 versus 0.61, Table 2). However, the interaction of the hydride with the second silyl does not change much on going from **4** to **6** (e.g., the longer Si···H distance of 2.083 Å increases only to 2.099 Å). Therefore, the substitution in the Cp ring radically changes the picture of Si–H interactions in this system: both silyls interact with the hydride, but a stronger Si···H interaction is significantly increased in the bulkier complex **6**. The higher-energy isomer of **6** is the silane σ -complex **7** with a virtually end-on silane coordination (Figure 7, right). Compared to **5**, it is in an earlier stage of Si–H activation characterized by a longer Rh–H distance (1.754 versus 1.632 Å), a shorter Si–H bond (1.599 versus 1.682 Å), and an increased $J(\text{H-Si})$ of –86.8 (Table 1). Interestingly, the energy difference between **6** and **7** is smaller than the difference between **4** and **5**: 4.2 kcal·mol⁻¹ versus 5.7 kcal·mol⁻¹ on the ΔE_e scale.

Stronger Si–H bonding with one of the silyl groups in **6** in comparison with **4** results in a larger Si–H coupling constant of –33.8 Hz. The coupling constant to the other silyl remains almost unaltered (–11.1 Hz), leading to a larger average $J(\text{H-Si})$ of –22.5 Hz. This value is in very good agreement with the experimental coupling constant |27.5| Hz determined by Taw, Bergman, and Brookhard,^{9b} thus lending further credibility to our calculations.

(34) Pleune, B.; Poli, R.; Fettinger, J. C. *J. Am. Chem. Soc.* **1998**, *120*, 3257.

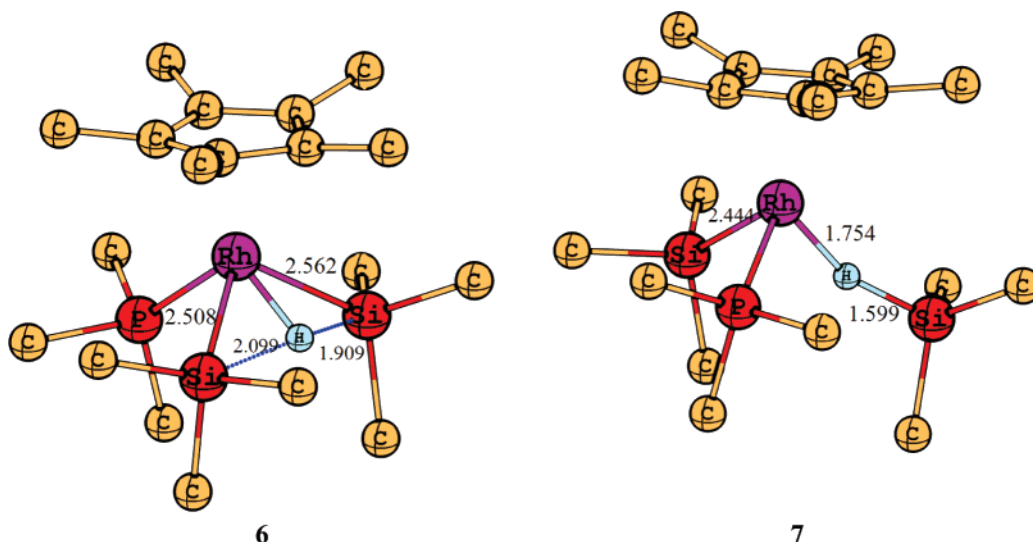


Figure 7. Structures of the pentamethylcyclopentadienyl-containing cations $[\text{Cp}^*\text{Rh}(\text{SiMe}_3)_2(\text{PMe}_3)\text{H}]^+$ (**6**) and $[\text{Cp}^*(\text{PMe}_3)\text{Rh}(\eta^2\text{-H-SiMe}_3)(\text{SiMe})]^+$ (**7**). Non-hydride hydrogen atoms are omitted for clarity. Distances are given in ångströms.

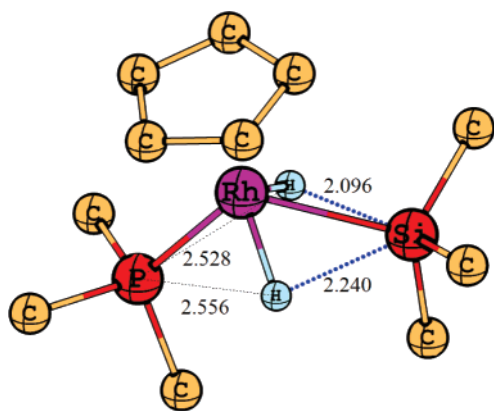


Figure 8. Structure of the cation complex $[\text{CpRh}(\text{SiMe}_3)(\text{H})_2(\text{PMe}_3)]^+$ (**8**). Non-hydride hydrogen atoms are omitted for clarity. Distances are given in ångströms.

In conclusion, comparison of the two forms of complex $[\text{Cp}^*\text{Rh}(\text{SiMe}_3)_2(\text{PMe}_3)\text{H}]^+$ with their unsubstituted analogues clearly establishes that substitution of the ring by methyl groups significantly increases the $\text{Si}\cdots\text{H}$ interaction. The driving force for this is the relief of steric strain coming from the elongation of the Rh-Si bond to the silicon center, which interacts stronger with the hydride.

5. $[\text{CpRh}(\text{SiMe}_3)(\text{H})_2(\text{PMe}_3)]^+$ (8**).** The compound $[\text{Cp}^*\text{Rh}(\text{SiMe}_3)(\text{H})_2(\text{PMe}_3)]^+$ was generated in solutions and studied by NMR.^{9b} It is an isoelectronic analogue of the complex $\text{Cp}^*\text{Rh}(\text{SiEt}_3)_2(\text{H})_2$ discussed above. However, the calculation of the model complex $[\text{CpRh}(\text{SiMe}_3)(\text{H})_2(\text{PMe}_3)]^+$ (**8**, Figure 8) showed that, unlike the isoelectronic bis(silyl) compound $\text{CpRh}(\text{SiMe}_3)_2\text{H}_2$ (**1**), it is severely distorted. The hydride ligands are shifted to the silyl group, away from the phosphine. The resultant Si-H distances (2.096 and 2.240 Å) are significantly shorter than the P-H distances (2.528 and 2.556 Å). Compared to related complexes **2–4**, a new feature is that one of the Si-H distances is shorter than the other. This suggests that complex **8** could be better referred to as a stretched silane σ -complex with an additional, weaker $\text{Si}\cdots\text{H}$ interaction. Consistent with this description is a slightly shorter Rh-H bond length for the “less interacting hydride” (1.575 versus 1.584 Å). Similar

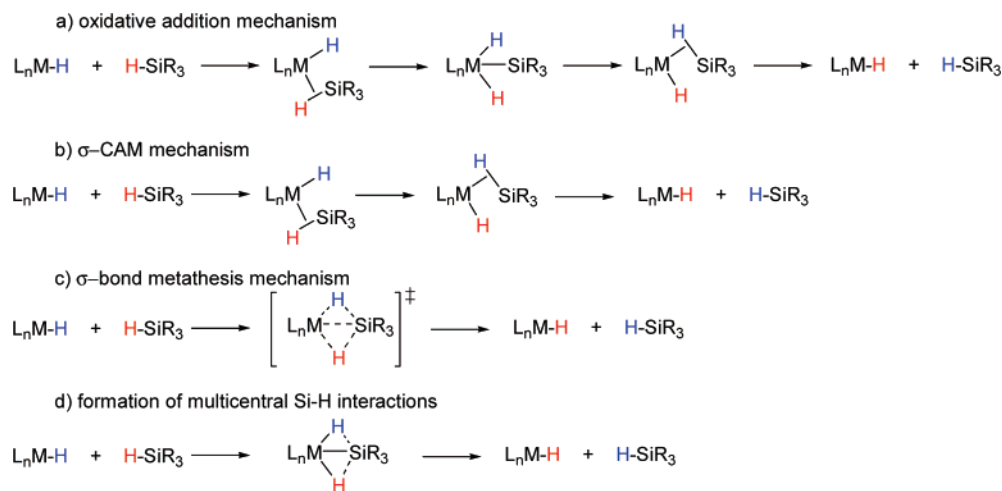
bonding situations have been previously observed in some silyl hydride complexes of ruthenium.³⁵

The real compound $[\text{Cp}^*\text{Rh}(\text{SiMe}_3)(\text{H})_2(\text{PMe}_3)]^+$ appears to be highly fluxional down to -80°C , so that no ^{29}Si satellite peaks could be observed in the ^1H NMR spectrum. Since the hydride signal is broad ($\nu_{1/2} \approx 50$ Hz), this brings about ambiguity in assigning the right structure by NMR (classical versus nonclassical). A degenerate exchange between two equivalent forms of a σ -complex ($[\text{Cp}^*\text{Rh}(\eta^2\text{-H}^a\text{-SiMe}_3)(\text{H}^b)(\text{PMe}_3)]^+ \rightleftharpoons [\text{Cp}^*\text{Rh}(\eta^2\text{-H}^b\text{-SiMe}_3)(\text{H}^a)(\text{PMe}_3)]^+$) would give rise to a small averaged $J(\text{H-Si})$ of 10–15 Hz (effectively buried in the width of the hydride signal) if the “real” Si-H coupling constant were on the order of 20–30 Hz.^{9b} Calculation of the $J(\text{H-Si})$ for the model complex **8** afforded values of -11.5 and -5.3 Hz (average -8.4 Hz). Again, the negative sign of the constants suggests the presence of direct Si-H bonding, which is further confirmed by significant Mayer indices (0.14 and 0.10, respectively). We therefore conclude that the lack of an observable Si-H coupling constant in complex $[\text{Cp}^*\text{Rh}(\text{SiMe}_3)(\text{H})_2(\text{PMe}_3)]^+$ is not due to the fluxionality. Rather, it stems from a small absolute value of this constant. Compared with the related $\text{CpRh}(\text{SiMe}_3)_2\text{H}_2$ (**1**), complex **8** has stronger Si-H interactions, evident from shorter Si-H distances, larger Mayer indices, and larger absolute values of $J(\text{H-Si})$ (Table 1).

Concluding Remarks

DFT calculations of silyl hydride complexes $[\text{Cp}(\text{Me}_3\text{E})(\text{X})\text{-Rh}(\text{SiMe}_3)_n]^+$ ($\text{E} = \text{Si}$, $\text{X} = \text{H}$, $n = 0$; $\text{E} = \text{Si}$, $\text{X} = \text{SiMe}_3$, $n = 0$; $\text{E} = \text{P}$, $\text{X} = \text{SiMe}_3$, $n = +1$; $\text{E} = \text{P}$, $\text{X} = \text{H}$, $n = +1$) revealed various degrees of interligand $\text{Si}\cdots\text{H}$ interaction, and strictly speaking, none of them have the oxidation state +5 for the metal. The minimum energy structure of compound $[\text{CpRh}(\text{SiMe}_3)_2\text{H}_2]$ is indeed suggestive of its description as a $\text{Rh}(\text{V})$ species, but calculations of the Si-H coupling constants and Mayer bond indices show the presence of weak residual $\text{Si}\cdots\text{H}$ interactions. Their silent feature is that the potential energy surface is extremely flat, making the formalism of oxidation states virtually senseless.

(35) Such interactions are called *SISHA* (Secondary Interactions between Silicon and Hydrogen Atoms) by some workers: Lachaize, S.; Sabo-Etienne, S. *Eur. J. Inorg. Chem.* **2006**, 2115.

Scheme 1. Mechanisms of Si–H Bond Activation, an Example of a Degenerate Hydride Exchange in the System $L_nMH/HSiR_3$ 

Complexes $[CpRh(SiMe_3)_3H]$ (**2**) and $[CpRh(SiMe_3)_2(SiEt_3)H]$ (**3**) have more profound interactions of the hydride with two *cis* silyl ligands. The strength of interligand $Si \cdots H$ bonding is controlled by the steric interaction between the bulky groups at rhodium (the Cp and silyls). The bulkier silyl $SiEt_3$ tends to interact with the hydride preferably, leading to a more effective relief of steric strain through the elongation of the Ru–Si bond. The complexes are highly fluxional due to a very facile hydride shift from one Si–Si edge to another. The transition state for the exchange in $[CpRh(SiMe_3)_3H]$ lies only $1.9 \text{ kcal} \cdot \text{mol}^{-1}$ (on the ΔG_{298}° scale) above the ground-state geometry and appears to have a η^2 -silane character, with one silyl interacting with the hydride more strongly than the two others. However, interactions with other silyls are not negligible and possibly help to reduce the barrier of exchange.

A similar bonding situation is found for the isoelectronic complex $[CpRh(SiMe_3)_2(PMe_3)H]^+$ (**4**), apart from the fact that it is not fluxional. Comparison of **4** with its ring-substituted analogue $[Cp^*Rh(SiMe_3)_2(PMe_3)H]^+$ (**6**) shows that the latter compound has a stronger $Si \cdots H$ interaction. Again, the interligand bonding is promoted by partial relief of steric hindrance in **6** due to elongation of the Rh–Si bond upon interaction of the silyl ligand with the hydride.

Finally, in the complex $[CpRh(SiMe_3)(H)_2(PMe_3)]^+$ the silyl interacts with both hydride ligands, but one interaction appears to be slightly stronger than the other. This complex is not fluxional. The lack of an observed Si–H coupling constant in the real compound $[Cp^*Rh(SiMe_3)(H)_2(PMe_3)]^+$ comes from a small magnitude of $J(H-Si)$. Compared with the isoelectronic $CpRh(SiMe_3)_2H_2$ (**1**), complex **8** has stronger $Si \cdots H$ interactions due to the localization of Si–H bonding on only one silicon center.

How can these relatively weak $Si \cdots H$ interactions be described in terms of the molecular orbital theory (MO)? It appears that a qualitative MO approach is limited in the case of highly delocalized σ -frameworks. For the related complexes $Cp(L)Fe(SiMe_3)_2(H)$, we have previously suggested considering them as adducts of the fragment $[Cp(L)Fe]^+$ with the anionic hypervalent silicon ligand $[Me_3Si-H-SiMe_3]^-$, leading to a four-center bond.¹⁴ The partial (but highly stretched) Si–H bonding then stems from an incomplete Si–H oxidative addition to iron, helping to avoid the unfavorable oxidation state +4. A similar description can be applied, in principle, to the related rhodium compounds $CpRh(SiMe_3)_3(H)$, $[Cp(Me_3P)Rh(SiMe_3)_2(H)]^+$, and $[Cp(Me_3P)Rh(SiMe_3)(H)_2]^+$ and can ac-

count, in principle, for the correlation between stronger Si–H bonds and longer Rh–Si distances. However, this approach increasingly loses its demonstrativeness in the case of complex $CpRh(SiMe_3)_2(H)_2$. In this case, both hydride ligands interact simultaneously and with comparable strength with both silyl ligands and move almost freely from one of them to the other in an extremely flat potential.

Very recently Lin *et al.* posed the question of “whether a two-step mechanism [of a metathetical process like that one in Scheme 1] could have an intermediate with the structural characteristics of a four-center species” and concluded that “the four-center transition state will never turn into an intermediate in the late-transition-metal systems, because the stabilization from the metal center is always provided by an occupied d orbital, thus turning a four-electron transition state into a six-electron transition state, which is a characteristic of a structure formed under oxidative addition”.³⁶ However, the rhodium complexes **1–4**, **6**, and **8** investigated in this work appear to have multicentral Si–H interactions,^{11a,14} which resemble to some extent interactions in the four-center transition state of a σ -bond metathesis reaction^{37,38} (Scheme 1, entry c). This happens due to the propensity of silicon to be hypervalent and also because it allows the system to avoid an unfavorably high oxidation state, which would arise if the donation of an electron pair from an occupied metal d-orbital were complete (i.e., a genuine six-electron situation). The conclusion of this work thus goes far beyond merely resolving the ambiguity in assigning an oxidation state of a metal in a series of rhodium complexes. More important is the finding that Si–H activation⁸ can result in a structure that is neither a classical silyl hydride (the product of complete oxidative addition of a Si–H bond in Scheme 1, entry a) nor a silane σ -complex (Scheme 1, entry b). Rather, complexes **1–4**, **6**, and **8** have more sophisticated, multicentral Si–H interactions (Scheme 1, entry d).

(36) Lam, W. H.; Jia, G.; Lin, Z.; Lau, C. P.; Eisenstein, O. *Chem. – Eur. J.* **2003**, *9*, 2775.

(37) (a) Gell, K. I.; Posin, B.; Schwartz, J.; Williams, G. M. *J. Am. Chem. Soc.* **1982**, *104*, 1846. (b) Watson, P. L.; Parshall, G. W. *Acc. Chem. Res.* **1985**, *18*, 51. (c) Thompson, M. E.; Baxter, S. M.; Bulls, A. R.; Burger, B. J.; Nolan, M. C.; Santarsiero, B. D.; Schaefer, W. P.; Bercaw, J. E. *J. Am. Chem. Soc.* **1987**, *109*, 203.

(38) Some examples of σ -bond metathesis reactions of silanes can be found in: (a) Tilley, T. D. *Acc. Chem. Res.* **1992**, *26*, 22. (b) Woo, H.-G.; Tilley, T. D. *J. Am. Chem. Soc.* **1989**, *111*, 8043. (c) Woo, H.-G.; Walzer, J. F.; Tilley, T. D. *J. Am. Chem. Soc.* **1992**, *114*, 7047. (d) Sadow, A. D.; Tilley, T. D. *Organometallics* **2003**, *22*, 3577.

This result also gets some significance in light of the very recent suggestion that activation and functionalization of X–Y bonds by late transition metal complexes goes via metathesis of σ -complexes in the coordination sphere of transition metals (σ -CAM mechanism in Scheme 1).³⁹ Although by no means do we intend to question the validity of this mechanism in general,⁴⁰ this work establishes that some of the earlier examples called to illustrate σ -CAM transformations of silanes (complexes **2**, **3**, **6**, **8**) have a more complicated bonding situation.

We hope our work sheds some new light on the true nature

(39) Perutz, R. N.; Sabo-Etienne, S. *Angew. Chem., Int. Ed.* **2007**, *46*, 2578.

(40) In general, we support the idea of exchange between σ -bond coordinated ligands and consider this work as complementary to the analysis given in ref 39.

of the high-oxidation-state species that may arise during metal-catalyzed transformations of organosilicon compounds.

Acknowledgment. This work was supported by the Spanish Ministry of Education and Science (Ramón y Cajal Program, grants CTQ2005-02698 and PCI2005-A7-0167) and Brock University.

Supporting Information Available: The description of basis set (in Gaussian format) and calculated atomic coordinates (in tabular form). This material is available free of charge via the Internet at <http://pubs.acs.org>.

OM070238X